Biomass and Bioenergy 149 (2021) 106077

Contents lists available at ScienceDirect

Biomass and Bioenergy

journal homepage: http://www.elsevier.com/locate/biombioe

Comparing continuous and batch operation for high-rate treatment of urban wastewater

Natalia Rey-Martínez, Aloia Barreiro-López, Albert Guisasola *, Juan A. Baeza

GENOCOV, Department of Chemical, Biological and Environmental Engineering, Universitat Autònoma de Barcelona, Spain

ARTICLE INFO

Keywords:
Anaerobic digestion
A-stage
COD fractionation
Energy recovery
High-rate

ABSTRACT

The water-energy nexus has changed the concept of wastewater treatment plants (WWTPs), which should move from energy consumers into energy neutral or even energy positive facilities. The A/B process aims at achieving self-sufficient energy WWTPs: organic matter is removed in the first step (A-stage) and derived to biogas production whereas autotrophic nitrogen removal is implemented in a second step (B-stage). This work compares two high-rate systems that can be used as A-stage in view of organic matter removal: a continuous high rate activated sludge (HRAS) reactor and a high-rate sequencing batch reactor (HRSBR). Both systems were operated with real urban wastewater at a short hydraulic retention time (2.5 h) and at short sludge retention time (SRT) of 1–2 d to minimize COD mineralization and to maximize organic matter diversion to methane production and, hence, energy recovery. The HRAS showed higher COD removal efficiencies and better energy recovery. On the other hand, the HRSBR was better to avoid undesired nitrification and provided lower COD mineralization for all the SRTs tested (ranging 20–48% for the HRSBR, and 41–58% for the HRAS). Then, the energy as methane recovered per unit of COD degraded was higher in the HRSBR. The HRSBR seems to be a good option, because the solids content in the effluent was similar for both systems and its COD removal efficiency can be further improved by optimizing the SBR cycle configuration.

1. Introduction

The activated sludge (AS) process is still the most commonly used technology for urban wastewater treatment since its first description in 1914 [1]. Although this technology is robust and provides a good effluent quality, it presents high operational costs and does not profit from the potential energy of the organic compounds present in sewage [2]. Moreover, nitrogen and phosphorus must be also removed to avoid eutrophication and oxygen depletion in water bodies. Conventional AS systems for nitrogen removal through nitrification/denitrification require high sludge retention times (SRTs), around 10–20 days, to ensure nitrification [3]. The major costs in these WWTPs are related to the energy consumption and sludge treatment: aeration can use about 60% of the total energy consumption [4], while sludge treatment and disposal can account for up to 40% [5].

However, these intensive energy requirements of conventional AS systems (0.3–0.6 $kWh \cdot m^{-3}$ [6]) are in contrast to the fact that wastewater is a valuable energy resource. Calculating the energy content of urban wastewater is not straightforward, but a value around 15 $kJ\ g^{-1}$ COD seems a conservative approach [7,8]. Therefore, the energy content of a typical influent with concentration 400 mg $COD \cdot L^{-1}$ would be around 1.7 $kWh \cdot m^{-3}$, which is 3–5 times higher than the energy needed for AS treatment. This value is even higher with less loaded wastewaters: Shizas and Bagley estimated that energy content of raw domestic sewage could exceed the electricity requirements to operate a conventional AS plant by a factor of nine [9]. Hence, these rough estimations reveal that WWTPs should not only aim at reducing their energy needs, but to become energy self-sufficient. Nowadays, the chemical energy contained in the influent can only potentially be recovered through the anaerobic digestion of the excess sludge. Alsayed et al. [10] estimated a range of potential values of energy recovery according to the efficiency of the primary settler. They estimated that about 15–35% of the influent COD could be converted to methane and subsequently to electricity in a Combined Heat and Power (CHP) equipment. This means that only 5–12% of the energy contained in the influent could be recovered as electricity, assuming an electricity efficiency of CHP technologies of 35% [11].

Urban WWTPs are currently energy-demanding facilities and thus

* Corresponding author.
E-mail addresses: Natalia.Rey@uab.cat (N. Rey-Martínez), aloiabarreiro@gmail.com (A. Barreiro-López), Albert.Guisasola@uab.cat (A. Guisasola), JuanAntonio.Baeza@uab.cat (J.A. Baeza).

https://doi.org/10.1016/j.biombioe.2021.106077
Received 15 November 2020; Received in revised form 24 March 2021; Accepted 18 April 2021
Available online 28 April 2021

novel approaches are needed for achieving a self-sustainable or even energy-positive WWTPs [4]. The four main bottlenecks to address are [10]: i) the amount of COD in the effluent (4–10% of the influent COD), ii) the excessive COD mineralization in the aeration tank (30–50% of the entering COD), iii) the limited anaerobic degradability or methane yield of the produced sludge (around 30% of the influent COD may not be completely digested to biogas), because long sludge retention times (SRTs) lead to poor digestibility and conventional AS including nutrient removal typically operate at long SRT $\geq$ 10 d. Finally, iv) the loss of COD as heat when using biogas to produce electricity using CHP technologies (10–23% of the influent COD). Thus, the utilisation of short-SRT systems with minimal mineralization and lower aeration needs seems a preferred option to boost energy recovery when removing organic matter from urban wastewaters.

The two-stage A/B process is a configuration targeting this goal [12] that has recently received more attention [13,14]. In the first step (known as A-stage), the objective is to maximize the capture of carbon through mostly physicochemical processes (adsorption, flocculation and coagulation) and to divert this sludge towards an anaerobic digestion system for maximising biogas production [15]. A-stage improvements for increasing COD removal through biosorption have been recently proposed [16], showing the applicability of these A/B processes. An A-stage system should operate at very short SRTs and short hydraulic retention times (HRTs) to minimize COD mineralization. The effluent of the first step is treated in the second step (stage B) through autotrophic biological nitrogen removal (BNR): partial nitritation and anaerobic ammonium oxidation (anammox) processes. Autotrophic BNR results in significant economic and energetic cost savings when compared to the conventional nitrification/denitrification process. The performance of the B-stage depends on the nature of the potential COD inlet and on the efficiency in solids removal at the A-stage. Moreover, the A-stage acts as a shock absorber of unexpected toxic loads that could be very detrimental for the B-stage [17].

The A-stage is usually designed as a continuous high rate activated sludge (HRAS) system under short SRT and HRT. For example, Jimenez et al. [18] studied the effect of SRT, HRT and dissolved oxygen (DO) on a HRAS pilot plant performance, while Ge et al. [19] evaluated the impact of SRT on nutrient removal using a HRAS pilot plant. A review of new alternatives for carbon redirection to improve the energy balance in WWTPs [20], demonstrated that HRAS is a good technology to redirect carbon in WWTPs. As an alternative to the continuous HRAS, a sequencing batch reactor (SBR) operating at similar HRT and SRT as the HRAS seems *a priori* also a good option because SBRs have some advantages compared with continuous systems: i) higher tolerance facing toxic or inhibitory compounds [21], ii) higher operation flexibility [22], iii) they retain sludge more effectively than continuous reactors because the supernatant is discharged only after the sludge has been settled [23] and iv) they can have lower installation costs and less space requirement because the process takes place in only one tank and thus avoids the settler.

Hence, the main objective of this work was to compare the performance in terms of COD removal and energy recovery of a continuous HRAS and a high-rate SBR (HRSBR) acting as an A-stage under the same SRT and HRT conditions and fed with real urban wastewater. On the basis of the obtained experimental results, the possible integration of both systems with a B-stage was discussed.

2. Materials and methods

2.1. Characteristics of the real wastewater

Two different real wastewaters were used in this work: primary settler influent (PSI) and primary settler effluent (PSE), both of them from a municipal WWTP (Rubí, Catalonia). Fresh wastewater was collected once a week and stored in a refrigerated tank at 5 °C. Table 1 summarizes the most important parameters of these wastewaters during the entire operation.

Table 1
Summary of wastewater characteristics for primary settler influent (PSI) and primary settler effluent (PSE).

Parameter	Influent average	
	PSI	PSE
TSS ($g{\cdot}L^{-1}$)	0.18 ± 0.17	0.08 ± 0.06
VSS ($g{\cdot}L^{-1}$)	0.16 ± 0.15	0.07 ± 0.05
Total COD ($mg{\cdot}L^{-1}$)	496 ± 214	359 ± 128
Particulate COD ($mg{\cdot}L^{-1}$)	239 ± 203	124 ± 93
Soluble COD ($mg{\cdot}L^{-1}$)	185 ± 54	157 ± 53
Colloidal COD ($mg{\cdot}L^{-1}$)	72 ± 26	76 ± 27
$N\text{–}NH_4^+$ ($mg{\cdot}L^{-1}$)	76 ± 13	65 ± 21
$P\text{-}PO_4^{-3}$ ($mg\ L^{-1}$)	9 ± 4	9 ± 3
pH	7.6 ± 0.2	7.6 ± 0.3

2.2. High-rate activated sludge (HRAS) reactor

The HRAS system consisted of a continuously stirred aerobic reactor (19 L) and a settler (27 L). It was operated at room temperature (18–22 °C) with an average influent flowrate of 165 L d^{-1} resulting in an HRT of 2.8 h. Daily sludge wastage was performed to maintain the SRT between 1 and 2 days. The external recycle from the settler to the reactor was 200 L d^{-1} resulting in an external recycle ratio R_{ext} of 1.2. The HRAS system was inoculated with sludge collected from the Rubí WWTP and was operated for 175 days treating PSE wastewater. The operation characteristics of each period are shown in Table 2. The HRAS reactor was managed with an on-line system based on an Advantech PCI-1711 I/O card and an industrial PC running the AddControl software developed in our research group. DO was measured with a HACH-CRI6050 DO probe and controlled around 1 mg L^{-1} by manipulating an on/off aeration valve. pH and temperature were monitored with a pH probe (HACH CRI5335) and a thermoresistance (Axiomatic Pt1000), respectively.

2.3. High-rate sequencing batch reactor (HRSBR)

The HRSBR was a stirred aerobic system with a working volume of 3.5 L and an exchange volume of 2.5 L. It was inoculated with sludge collected from the same WWTP and the HRT was fixed at 2.5 h. Daily sludge wastage was performed to maintain an SRT between 1 and 2 days. The reactor was monitored for oxygen, pH and temperature and controlled with a PLC. The SBR was operated at a controlled temperature of 25 ± 1 °C. pH was not controlled, however its value was maintained in the range 7.5–8.6 during the entire operation. DO was controlled between 5 and 6 mg L^{-1} by manipulating an on/off aeration valve during the start-up and, afterwards, the set point was decreased to 3 mg L^{-1} and maintained at this value during the rest of the operation.

The operation (253 days) was divided into different periods according to the operational conditions and the cycle configuration for each period is reported in Table 3. The HRSBR was fed with PSI during periods I and II and with PSE for the rest of the periods.

2.4. Anaerobic digestion batch tests

The biochemical methane potential (BMP) of the sludge purged in both systems was studied through anaerobic batch digestion tests. BMP

Table 2
Operational conditions for each period of the HRAS.

Period	Days (d)	Carbon source	Purge flow ($L{\cdot}d^{-1}$)	SRT (d)
I	0–24	PSE	5	2.5 ± 0.2
II	26–87	PSE	3.5	2.1 ± 0.6
III	89–175	PSE	2.5	1.2 ± 0.6

Table 3
Operational conditions for each period of the HRSBR.

Period	Days (d)	Carbon source	Purge flow ($L \cdot d^{-1}$)	SRT (d)	Cycle length (min)	Reaction phase (min)	Settling phase (min)	Discharge phase (min)
I	0–30	PSI	modified to obtain a constant SRT	1.8 ± 0.9	106	75	30	1
II	58–105	PSI	0.576	1.2 ± 0.5	116	85	30	1
IIIA	107–191	PSE	0.576	2.2 ± 1.0	116	85	30	1
IIIB	194–231	PSE	0.576	1.3 ± 0.8	116	85	30	1
IV	236–253	PSE	0.993	1.0 ± 0.3	116	85	30	1

assays were performed in 160 mL glass bottles (125 mL of working volume) with rubber stoppers and screw caps according to Angelidaki et al. [24]. The inoculum used in the tests was obtained from the anaerobic digester of the Rubí WWTP and was pre-incubated at 37 °C in order to deplete the residual biodegradable organic matter. All tests were performed by triplicate in an incubator at T = 37 °C and manually mixing of the bottles once a day. A substrate to inoculum (S/I) ratio of 1 (on VS basis) with 2 $gVS \cdot L^{-1}$ of inoculum was used. Negative control assays with only inoculum and MilliQ water were conducted in parallel to measure the background BMP from the inoculum and this was subtracted from the test prior to parameter estimation. Additionally, a positive control with cellulose as substrate was performed to confirm the activity of the inoculum. The liquid phase and the headspace of the bottles were flushed with nitrogen to provide anaerobic conditions. A pressure transducer was used to measure the pressure increase. The biogas was sampled regularly and its composition was determined by gas chromatography. The moles of methane were calculated by the ideal gas law (Equation (1)):

$$\text{moles}CH_4 = \frac{P_T \cdot x_{CH_4} \cdot V_{headspace}}{R \cdot (T + 273)} \quad (1)$$

where P_T is the total pressure measured by the transducer (mmHg), x_{CH4} is the methane molar fraction, $V_{headspace}$ is the headspace volume (mL), R is the ideal gas constant (62,320 mmHg $mL \cdot mol^{-1} \cdot K^{-1}$) and T is the temperature (°C). Then, the corresponding volume of methane can be calculated and converted to standard temperature and pressure conditions (0 °C and 1 atm).

2.5. Specific analytical methods and calculations

Samples for phosphorus and ammonium, nitrate and nitrite were filtered through 0.22 μm filters (Millipore). Phosphorus concentration was measured with a phosphate analyser (PHOSPHAXsc, Hach Lange) based on the vanadomolybdate yellow method. Ammonium nitrogen was analysed with an ammonium analyser (AMTAXsc, Hach Lange), based on the potentiometric determination of ammonia. Analyses of nitrite and nitrate samples were performed with ionic chromatography (DIONEX ICS-2000).

Influent and effluent COD fractions were measured according to Jimenez et al. [18]. Particulate COD (COD_P) was the difference between total COD (COD_T) and the COD filtered through a 1.5 μm filter (COD_F). The soluble COD (COD_S) was the flocculated and filtrated COD (COD_{ff}) as defined by Mamais et al. [25]. Colloidal COD fraction (COD_C) was defined as the difference between COD_P and COD_S. These COD fractions were measured using COD kits (Lovibond Vario LR and Vario MR) and a spectrophotomer (Photometer system MD100 Lovibond). Total suspended solids (TSS) and volatile suspended solids (VSS) were analysed according to APHA [26].

Biogas composition (CH_4 and CO_2) was analysed with a Hewlett Packard gas chromatograph (HP 5890) equipped with a thermal conductivity detector (TCD) and a Supelco Porapack Q (250 °C) 3 m x 1/8" column. Helium was the carrier gas at 338 kPa, and the oven, injector and detector temperatures were 70, 150 and 180 °C respectively. A total sample volume of 100 μL was used for chromatography.

The observed yield (Y_{obs}) under different SRT conditions was calculated using the experimental biomass production (P_X, equation (2)).

$$P_X = Q_p \cdot X_p + Q_e \cdot X_e - Q_{in} \cdot X_{in} \quad (2)$$

Where Q_p, Q_e and Q_{in} are the flowrates of purge, effluent and influent ($L \cdot d^{-1}$) and X_p, X_e and X_{in} are the VSS concentrations in the purge, in the effluent and in the influent ($gVSS \cdot L^{-1}$).

The experimental observed yield (Y_{obs}, $gCOD \cdot g^{-1}COD$) was calculated with equation (3).

$$Y_{obs} = \frac{P_X \cdot 1.416}{Q_{in} \cdot (COD_{in} - COD_{out})} \quad (3)$$

where 1.416 is a stoichiometric factor converting VSS into COD ($gCOD \cdot g^{-1}VSS$), Q_{in} is the influent flowrate ($L \cdot d^{-1}$) and COD_{in} and COD_{out} are the COD concentrations in the influent and effluent respectively ($mgCOD \cdot L^{-1}$).

Two different energy recovery indices were used, the methane recovery index (MRI) and the energy recovered index (ERI). MRI was calculated as the COD content of the methane recovered (g COD_{CH4}) per gram of COD removed (g COD_{REM}) using equation (4). MRI is function of the mineralization degree in the reactor and the digestibility of the produced solids. This value was calculated as:

$$MRI = \frac{gCOD_{CH4}}{gCOD_{REM}} = Y_{obs}\left[\frac{g\,VSS}{g\,COD_{REM}}\right] \cdot BMP\left[\frac{NLCH4}{gVSS}\right] \cdot ConvFact\left[\frac{gCOD_{CH4}}{NLCH4}\right] \quad (4)$$

where ConvFact was calculated as function of the T and P as 2.86 g COD_{CH4}/ NL CH_4

ERI was calculated as the energy that could be obtained in the produced methane (kJ_{CH4}) per energy in the influent (kJ_{INF}) using equation (5). ERI includes the efficiency of the CHP, the energy content of the influent wastewater and the percentage of COD removed. The theoretical energy yield of methane is 13.9 kJ $g^{-1}CH_4$ [8] and a CHP efficiency of 35% was assumed [11]. The energy content of the COD in the influent wastewater was assumed as 15 kJ g^{-1} COD, according to literature [7,8].

$$ERI = \frac{kJ_{CH4}}{kJ_{INF}} = \frac{CH4\ \ prod\ [g\ CH4] \cdot Energy\ \ CH4\left[\frac{kJ}{g\ CH4}\right] \cdot CHP_{Efficiency}}{Influent\ \ load\ [gCOD_{INF}] \cdot Energy\ \ of\ \ Influent\left[\frac{kJ}{g\ COD_{INF}}\right]} \quad (5)$$

3. Results and discussion

3.1. Continuous HRAS system performance

The continuous HRAS system was operated for 175 days under two

different SRTs and real PSE as feed. During the start-up (period I), the average COD_S removal efficiency was 66 ± 6%. Fig. 1 shows the average values of influent/effluent COD_T and the sludge volume index (SVI) measured for periods II and III. The COD_T in the effluent was not affected by the reduction of the SRT from 2 d (period II) to 1 d (period III). In fact, the COD_T removal efficiencies were 70 ± 16% and 65 ± 15% respectively. The slight increase in the effluent COD_T concentration from period II to period III was probably due to the 18% increase in the influent COD_T (Fig. 1).

The settleability of the sludge in the HRAS reactor was never good as can be deduced from the high SVI values (Fig. 1), being 568 ± 329 mL g VSS^{-1} the average value during the entire operation. The settleability problems led to an extremely low solids concentration (Fig. 2): the VSS reached values around 0.13 g L^{-1} during period III. In fact, from day 140–168 of operation, the purge had to be turned off because of this low VSS concentration. Settleability issues are very relevant when implementing novel technologies at low SRT and, in this case, a settler with higher surface than the conventional ones would be needed after the continuous HRAS reactor. In this sense, Rahman et al. [27] proposed a settler three times bigger than the reactor when operating A-stage and high-rate contact-stabilisation systems. Jimenez et al. [18] did not report settleability problems working with a biological reactor of 260 L and a sedimentation tank of 280 L.

3.2. HRSBR performance

The HRSBR was operated for 253 days under different conditions (Table 3). Period I corresponds to the start-up of the reactor. The objective of this period was operating with a constant SRT of 2 days, but this required a daily modification of the purge flow, which could lead to an unstable operation. Thus, it was decided to maintain a constant purge flow in the subsequent periods II and III (0.576 L d^{-1} and 0.993 L d^{-1} respectively) and, thus, the SRT fluctuated in a range of 1.2–2.2 days. Period III was divided into IIIA and IIIB because there was an incident and the reactor had to be inoculated again with biomass from the previous purges, which had been stored at 4 °C. Finally, the purge flow was maintained at 0.993 L d^{-1} in period IV and the system operated at a SRT of 1.0 ± 0.3 days. The evolution of the solids in the HRSBR is presented in Fig. 3. It is worth mentioning that biomass attachment to the walls of the reactor was observed in periods I and II. Therefore, the decrease in the solids concentration during period II might be unreliable. The walls of the reactor were scratched once a week from period IIIA onwards in order to detach this biomass. Attached biomass can distort the total solids concentration in the reactor and consequently the real value of the SRT, being higher than desired. The solids concentration increased during period IIIA because of the detachment of the biomass grown on the walls of the reactor, however TSS and VSS diminished again during periods IIIB and IV when the SRT was decreased from 2.2 ± 1.0 d (period IIIA) to 1.3 ± 0.8 and 1.0 ± 0.3 d respectively.

Fig. 4 shows the evolution of the COD_T and the average SVI in the HRSBR operation. The effluent COD_T was below 200 mgCOD·L^{-1} during periods I, II and IIIA, and it increased around 300 mgCOD·L^{-1} for periods IIIB and IV. High effluent COD_T is linked to the poor settleability of the sludge (SVI reached 300–500 mL·g^{-1}VSS). The fractionation of the effluent COD (Fig. 5) shows that during periods IIIB and IV the effluent COD_P increased. This fraction is strongly related to the sludge settling characteristics [28].

3.3. Comparison of effluent quality and carbon removal in both systems

The effluent quality of both systems was evaluated in terms of solids concentration and effluent COD fractions (Table 4 and Fig. 6 respectively). The average effluent TSS in each reactor were similar but the average SVI for the HRAS sludge (568 ± 329 mL g^{-1} VSS) was much higher than the observed for the HRSBR sludge (206 ± 192 mL g^{-1} VSS), indicating that the former had worse settleability properties (Table 4).

Fig. 6 shows the average values of the different COD fractions as function of the SRT in both experimental systems. In the case of the HRAS reactor, the effluent COD_T, COD_F and COD_P concentrations increased (23.5, 11.7 and 31.2% respectively) when SRT decreased from 2.1 d to 1.2 d. COD_C had similar concentrations between 8 and 15 mg COD·L^{-1} in all cases and COD_S was below 50 mg COD·L^{-1} for both SRT. Similar results of the effect of SRT on the effluent COD fractions was also observed by Rahman et al. [29] when comparing continuous systems treating raw wastewater.

Regarding the HRSBR operation, effluent COD_T, COD_F and COD_P increased when SRT decreased, except for SRT = 1.2 d (period II). This fact could be explained by the attached biomass on the walls of the reactor, which resulted in an effective SRT higher than that calculated considering only planktonic biomass. The rest of the COD fractions were less affected by the SRT: COD_S was in the range of 59.4–80.8 mgCOD·L^{-1} in all cases whereas COD_C had a minor role due to the low influent concentrations (14.5–21.2% of influent COD_T) (Table 1).

COD removal efficiencies for both systems are shown in Table 5. The HRAS system showed lower COD removal efficiency (from 70 to 65% COD_T removal) when decreasing the SRT from 2.1 to 1.2 d. Higher variations were observed for the HRSBR. If the results of periods I and II are discarded due to the problems of biomass attached to the reactor walls, a clear decreasing trend of COD removal is observed when SRT decreases. For example, the COD_T removal efficiency decreased from 54 to 15% when the SRT decreases from 2.2 to 1 d. Thus, the lower the SRT, the higher the effluent COD_T. Understanding the behaviour of the removal efficiencies of each individual COD fraction is not straightforward since many non-controlled interactions happen (from hydrolysis to aggregation). Moreover, the values of these fractions in the reactor are dynamic and, thus, some positive or negative accumulation of these fractions may occur. Removal efficiencies lower than 50% were achieved for COD_P during the entire operation. In fact, negative COD_P removal efficiencies were obtained when SVI increased and the solids content in the reactor was reduced (periods IIIB and IV corresponding to

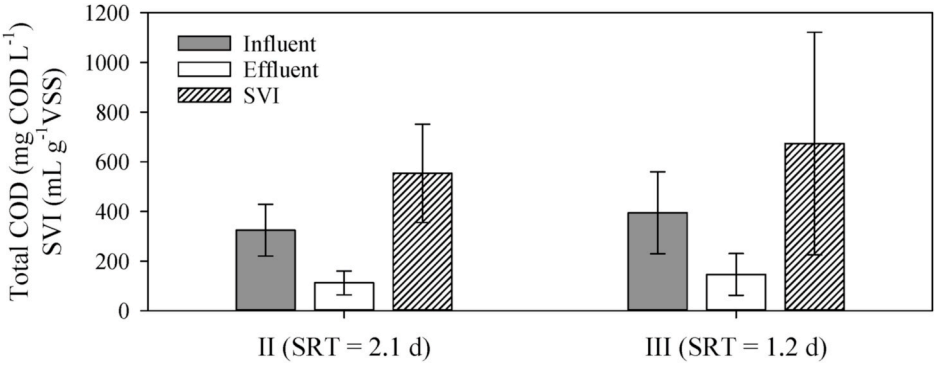

Fig. 1. HRAS operation. Average influent and effluent COD_T and SVI in periods II and III.

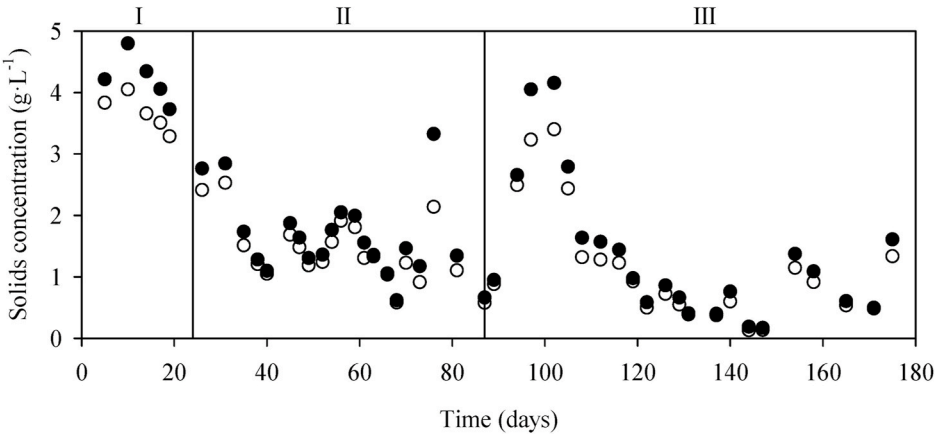

Fig. 2. HRAS operation: suspended solids in the reactor. (●) TSS and (○) VSS.

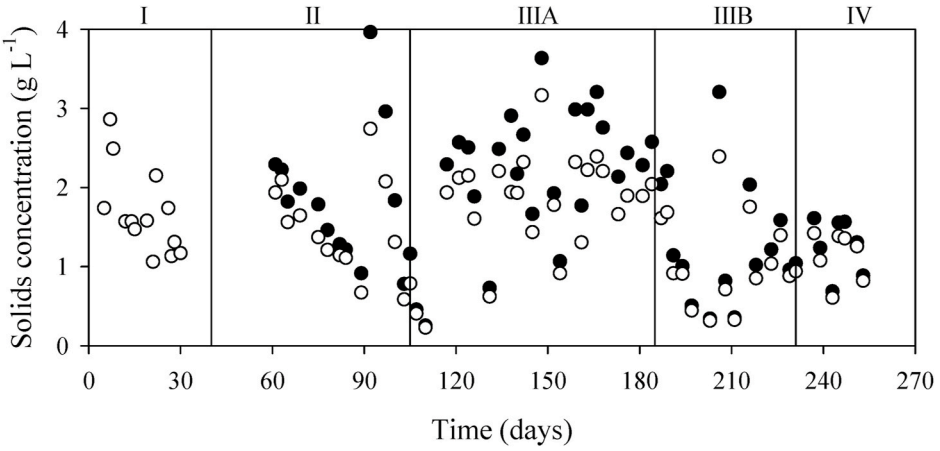

Fig. 3. HRSBR operation: suspended solids in the reactor. (●) TSS and (○) VSS.

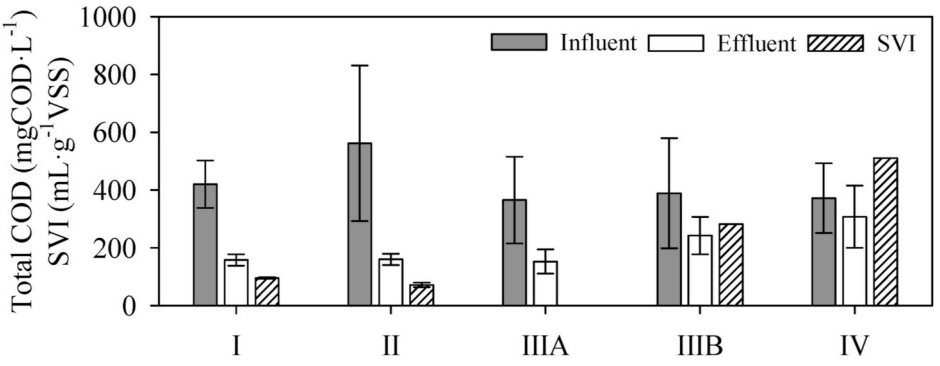

Fig. 4. HRSBR operation: COD_T in the influent and in the effluent and SVI.

the lower SRT tested of 1 d). That led to a high effluent COD_P value, which was transitorily higher than the influent COD_P. A decrease in the COD_C removal efficiency during the same periods (Table 5) was also observed. Therefore, the efficiency removal of COD_P and COD_C decreased in parallel to the decrease in the SRT but with limited impact on the COD_S. Faust et al. [30] reported that a lower amount of extracellular polymeric substances was detected at lower SRTs. Thus, bioflocculation, the mechanism responsible for removing particulate and colloidal COD from wastewater [31], was unfavourable at low SRT values. Jimenez et al. [18] obtained a similar trend, the efficiencies for COD_P and COD_C removal decreased from 70% to around 40% and 60% respectively when the SRT decreased from 2 to 1 day.

The presence of either solids or organic matter in the influent of a B-stage can decrease its performance [17]. Thus, the effluent of the high-rate system should not contain a significant organic load to the B-stage process. Otherwise, this organic matter would promote the growth of heterotrophic bacterial population, which would compete with the autotrophic bacteria for the electron acceptor (i.e. mostly nitrite) resulting in a limitation of the autotrophic nitrogen removal [32, 33] and an increase of the aeration requirements. Considering this COD removal criterion, the effluent of the HRAS reactor was more adequate than that from the HRSBR, as the COD_T removal efficiencies were systematically higher in the former case. Moreover, a higher impact of SRT on COD removal efficiencies was observed for the HRSBR (Table 5). The

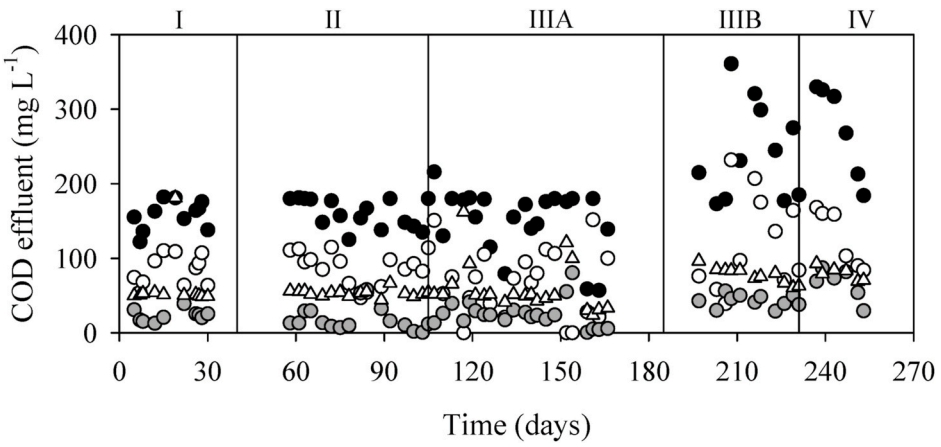

Fig. 5. HRSBR operation: Effluent COD fractionation: Total (●), particulate (○), colloidal (●) and soluble (Δ).

Table 4
Total suspended solids concentration in the reactor and in the effluent for both systems.

System	TSS reactor ($g \cdot L^{-1}$)	TSS effluent ($g \cdot L^{-1}$)	SVI ($mL \cdot gVSS^{-1}$)
HRAS			
I (start-up)	2.5 ± 0.2	0.059 ± 0.039	171
II	2.1 ± 0.6	0.060 ± 0.068	553 ± 198
III	1.2 ± 0.6	0.075 ± 0.069	673 ± 448
HRSBR			
I	1.8 ± 0.9	0.097 ± 0.048	95 ± 3
II	1.2 ± 0.5	0.134 ± 0.058	71 ± 8
IIIA	2.2 ± 1.0	0.070 ± 0.040	–
IIIB	1.3 ± 0.8	0.081 ± 0.038	282
IV	1.0 ± 0.3	0.097 ± 0.040	510

periods with the same SRT for both systems, as for example when SRT was around 2 days (period II of the HRAS and period IIIA of the HRSBR), had similar COD_S removal efficiency (60 vs. 57%). However, higher COD_P removal efficiency was obtained for the HRAS (70 vs. 25%), showing the higher capacity of separation of particulate compounds in the continuous HRAS.

3.4. COD_T mass balances

COD_T mass balances were performed at different SRTs for both systems using the steady-state data (Fig. 7A and B). In addition, taking into account the floc formation limitations usually found in high-rate systems [34], which lead to high biomass concentration in the effluent, the COD mass balance distribution in a perfect settling scenario (no solids in the effluent) was also evaluated. Fig. 7C and D shows this scenario considering that all of the effluent biomass could be redirected to the anaerobic digestion. Mineralization was estimated as in Akanyeti et al. [2], i.e. the COD fraction required to close the COD mass-balance.

Fig. 7A and B shows the COD distribution for the continuous HRAS and for the HRSBR. The data of the mineralization of the COD and the COD distribution was very dependent on the effluent solids. These variable concentrations of effluent solids can be attributed to a settling issue rather than a problem with the reactor configuration and, hence, the discussion of Fig. 7C and D becomes more meaningful.

The COD distribution obtained in the perfect settling scenario (Fig. 7C and D) was estimated assuming that: i) effluent COD_S was the only effluent COD fraction and ii) the experimental solids in the effluent were considered as part of the purge and the COD content in these solids was estimated using the same procedure as in the purge and with the stoichiometric factor 1.416 $gCOD \cdot g^{-1}VSS$.

The extent of mineralization in the HRAS system was important (Fig. 7C), where values around 41–58% were observed. These values are in the range obtained by Jimenez et al. [18] and Akanyeti et al. [2] at SRT of 1 d. Moreover, the fraction of the inlet COD directed to the purge decreased from 34% to 30% when the SRT decrease from 2 to 1 d. Previous works [2,18] reported carbon redirection improvement when lowering the SRT. Our observation (i.e. similar COD distribution independently of the SRT) could be attributed to the SRT range tested, always higher than 1 day. In fact, Jimenez et al. [18] and Rahman et al. [29] did not observe differences between the COD distribution for 1–2 d SRT, and a clear difference was only observed at SRT below 0.5 d. Akanyeti et al. [2] also worked with SRT below 1 d (0.25, 0.5 and 1 d), obtaining a mineralization of 27%, 41% and 54%, respectively.

Regarding the HRSBR, a decrease in the SRT implied an increase of the COD redirected to the purge, up to 62% when the SRT was 1 d. Consequently, the COD fraction in the effluent decreased considerably: the values obtained in this hypothetical scenario were in the range of 16–19%, whereas the values reached in the real mass balance were in the range 42–74%. The COD redirected to purge obtained in this work at an SRT of 1 d (62%) was higher than the values observed in other studies with continuous systems operating at even lower SRTs. For example, Rahman et al. [27] observed percentages of COD in purge around 43% only at SRT of 0.3 d. The extent of mineralization was lower in the HRSBR (20–48%) than in the continuous HRAS system (41–58%), with the highest difference for SRT = 1d: 20% for HRSBR and 58% for HRAS. Then, mineralization in the HRSBR was lower than that obtained by Jimenez et al. (2015) for the same SRT (60%). However, when the authors worked at shorter SRTs (0.3–0.1 d) the mineralization decreased until 20%, which is the value obtained for the HRSBR at SRT = 1d. As a conclusion, the HRSBR allowed a better control of the extent of mineralization process, which means that there was more COD in the purge and available for redirection to anaerobic digestion.

3.5. Observed biomass growth yield (Y_{OBS})

The values of Y_{OBS} calculated for each SRT are presented in Table 6. Y_{OBS} seems to be higher at high SRT in the HRAS. The start-up (period I) was the period with the highest SRT value (2.5 d), and with highest Y_{OBS} (1.05 ± 0.38 $gVSS \cdot g^{-1}COD$). Values higher than one are not possible when considering only biological processes. However, higher Y_{OBS} values make sense if other non-biological processes such as adsorption occur. There may be a fraction of COD, which is not degraded, that is adsorbed in the solids of the effluent, leading to the overestimation of VSS. Ge et al. [19] also observed the same behaviour operating a lab-scale HRAS system with Y_{OBS} values between 10 and 13 $gVSS \cdot g^{-1}COD$ for SRT of 2–3 d and 3–6 $gVSS \cdot g^{-1}COD$ for SRT of 0.5–1 d (Table 6). In contrast, in the HRSBR and at higher SRTs (2.2 d), the Y_{OBS} (0.58 ± 0.34 $gVSS \cdot g^{-1}COD$) was lower compared than at short SRT

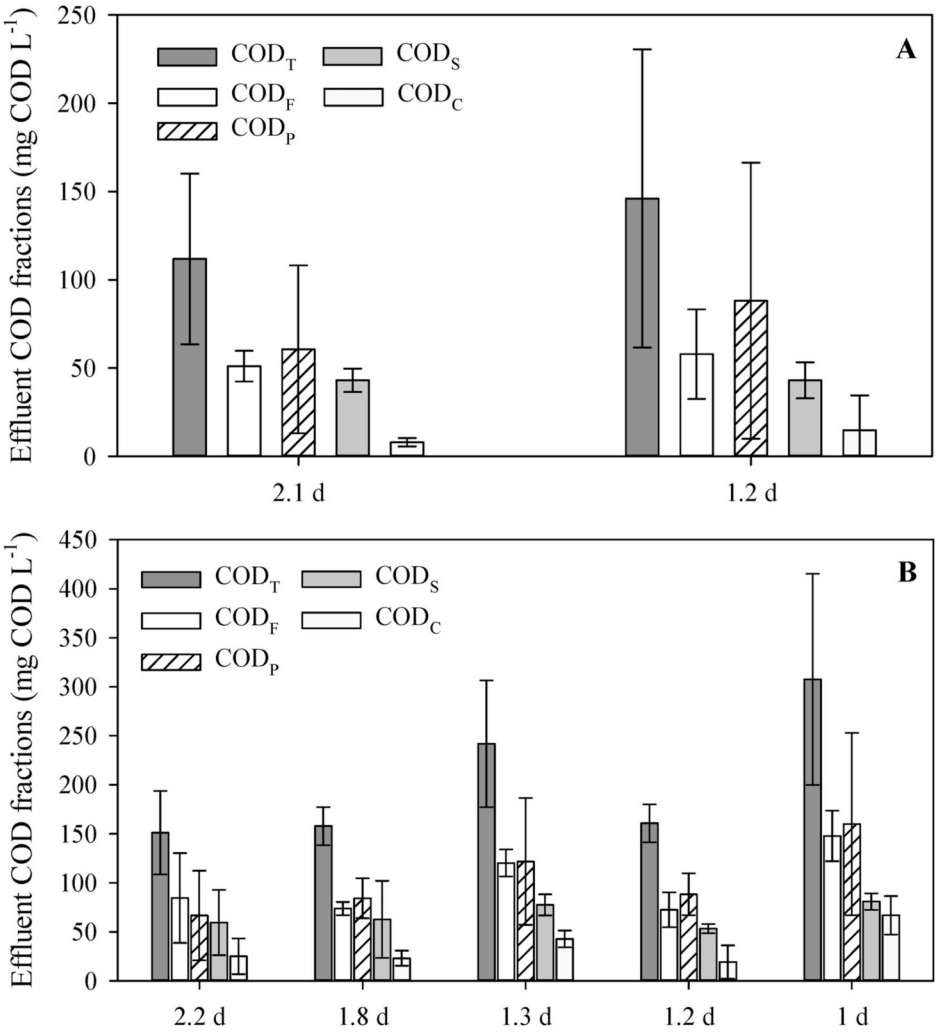

Fig. 6. Average COD fractionation in the effluent of A) HRAS and B) HRSBR.

Table 5
COD removal efficiencies (%) for both high rate systems.

	SRT (d)	Period	COD_T	COD_F	COD_P	COD_S	COD_C
HRAS	Start up	I	–	–	–	–	–
	2.1 ± 0.6	II	70 ± 16	64 ± 5	70 ± 32	60 ± 7	77 ± 7
	1.2 ± 0.6	III	65 ± 15	63 ± 18	66 ± 23	55 ± 17	71 ± 22
	1.8 ± 0.9	I	60 ± 10	68 ± 5	38 ± 36	58 ± 27	72 ± 17
HRSBR	1.2 ± 0.5	II	66 ± 13	72 ± 8	44 ± 39	73 ± 7	67 ± 27
	2.2 ± 1.0	IIIA	54 ± 17	62 ± 9	25 ± 99	57 ± 12	57 ± 20
	1.3 ± 0.8	IIIB	27 ± 19	50 ± 4	–	51 ± 10	42 ± 15
	1.0 ± 0.3	IV	15 ± 27	43 ± 5	–	47 ± 10	33 ± 18

conditions (1 d) with Y_{OBS} values of 1.35 ± 0.54 gVSS·g^{-1}COD. This effect of SRT on the Y_{OBS} was similar to the observed by Jimenez et al. [18] and Rahman et al. [29] (Table 6). It is worth mentioning that, in the case of the HRSBR, the values of Y_{OBS} for periods I and II were not considered due to the observation of biomass attachment to the walls of the reactor.

3.6. Nutrient removal

Fig. 8 shows the nitrogen and phosphorus concentrations in the influent and effluent of the continuous HRAS system and the HRSBR during the entire operation. Some nitrification was observed in the case of continuous HRAS reactor (Fig. 8A): ammonia removal efficiencies of 53 ± 11% and 47 ± 17% were obtained during periods I and II respectively. However, from day 115 until day 145, ammonia removal efficiency decreased down to 10 ± 5%. This ammonia removal could be attributed to assimilation for microbial growth rather than to nitrification. The amount of nitrogen incorporated into the biomass during the cellular synthesis (Table 6) was estimated with mass balances, considering the COD removal values, the sludge yield and the typical stoichiometric factor of 0.086 g N·g^{-1}COD reported by Henze et al. [35] for modelling studies. It can be inferred that 31% and 23% of the influent nitrogen was removed due to heterotrophic growth during periods I and II. The assimilative nitrogen uptake was higher in period I; however, ammonia assimilation in this case could be overestimated since it was considered that all the solids in the effluent were biomass and, as discussed above, there was an unaccounted fraction of adsorbed COD. The occurrence of nitrification in periods I and II at SRT values of 2.5 days and T = 20 °C was unexpected. However, the proliferation of some nitrifiers as a biofilm grown on the reactor walls could explain the detection of some nitrification activity. On the other hand, nitrification was not detected during period III (SRT = 1 d) onwards due to the periodic scratching of the walls. Then, the percentage of nitrogen

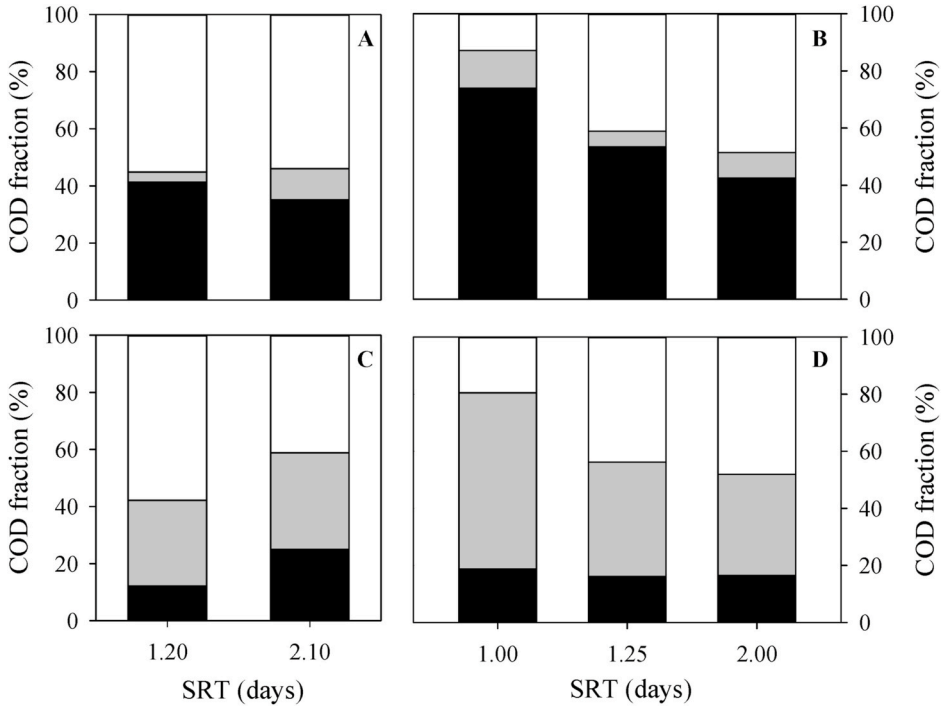

Fig. 7. Ouput COD distribution as a fraction of influent COD at different SRT conditions for A) HRAS and B) HRSBR. C) and D) correspond to HRAS and HRSBR in the perfect settling scenario. Effluent (■), purge (▭) and mineralization (□).

Table 6
Observed yield as a function of SRT.

System	Period	SRT (d)	Y_{obs} (gCOD·g^{-1}COD)	Y_{obs} (gVSS·g^{-1}COD)	$\frac{N_{growth}}{N_{influent}}$ (%)	N-removal (%)
HRAS	III	1.2 ± 0.6	0.53 ± 0.35	0.37 ± 0.25	22 ± 19	11 ± 4
(This study)	II	2.1 ± 0.6	0.92 ± 0.80	0.65 ± 0.56	23 ± 16	19 ± 7
	I	2.5 ± 0.2	1.48 ± 0.54	1.05 ± 0.38	31 ± 4	32 ± 9
HRSBR	IV	1.0 ± 0.3	1.91 ± 0.77	1.35 ± 0.54	24 ± 2	6 ± 2
(This study)	II	1.2 ± 0.5			20 ± 6	20 ± 10
	IIIB	1.3 ± 0.8	0.83 ± 0.43	0.59 ± 0.31	13 ± 7	4 ± 2
	I	1.8 ± 0.9			21 ± 9	22 ± 6
	IIIA	2.2 ± 1.0	0.81 ± 0.49	0.58 ± 0.34	18 ± 10	6 ± 3
HRAS		0.5		0.47 ± 0.11		
[18]		1.0		0.38 ± 0.08		
		2.0		0.33 ± 0.10		
CSTR		0.2	0.54 ± 0.06			
[29]		0.8	0.47 ± 0.08			
		2.2	0.45 ± 0.13			
HRAS		0.5–1		3–6		
[19]		2–3		10–13		

attributed to growth was higher than the nitrogen removal efficiency (Table 6).

In the case of the HRSBR, the average nitrogen removal was 21 ± 8% for periods I and II, however in the subsequent periods this value decreased down to 7 ± 1% (Fig. 8B). In this case, 18% of the influent nitrogen was removed via biomass assimilation or adsorption for the higher SRT tested (2 d). A 24% of the nitrogen influent was removed by heterotrophs growth when SRT was 1 d (Table 6).

Nitrification is neither expected nor desired in a high rate system, as only COD should be removed during this step. It was only observed in the HRAS when the growth of a biofilm in the reactor walls was not prevented. The significance of the reactor walls is an inherent problem only for lab-scale reactors and it is not expected to be important at full-scale systems.

Regarding phosphorus, the slight phosphate consumption observed could be due to assimilation during microbial growth for both systems. P-removal efficiencies of 9.5–12% were obtained in HRAS whereas higher values between 7 and 28% were obtained in the HRSBR (Fig. 8C and D respectively). The oscillations in the influent concentration were due to variations of the real wastewater.

3.7. Methane yield and hydrolysis constants

Anaerobic digestion assays of the sludge generated in both systems and in periods with different SRT were performed (Fig. 9 and Table 7). The highest BMP (307.8 ± 6.7 L CH_4·kg^{-1}VS-added) was obtained for

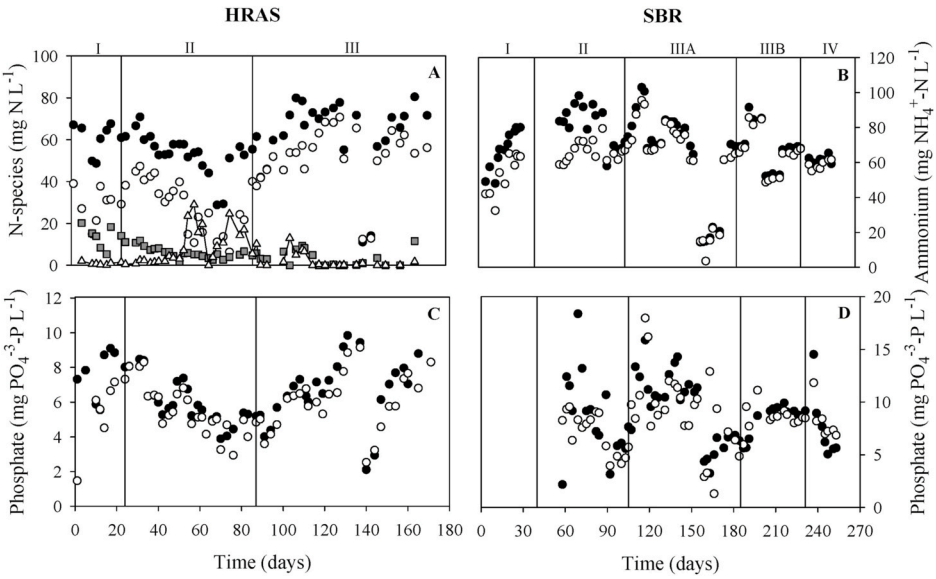

Fig. 8. Ammonium concentration in the influent (●) and in the effluent (○) A) for HRAS and B) for HRSBR. Nitrite (■) and nitrate (Δ) concentrations in the effluent for HRAS. Phosphate concentration in the influent (●) and in the effluent (○) C) for HRAS and D) for HRSBR.

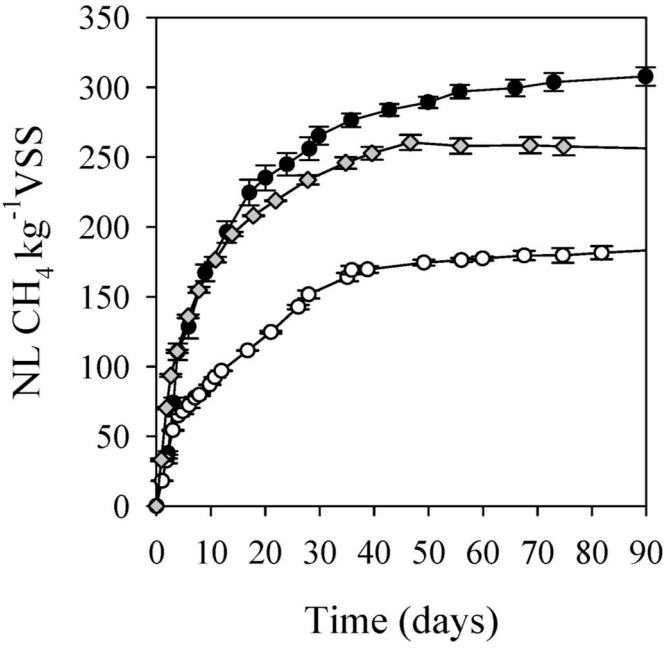

Fig. 9. Cumulative BMP from mesophilic anaerobic digestion batch tests for different SRTs sludge. HRAS: 1.2 d (◆). HRSBR: 2 d (○), 0.8 d (●).

Table 7
Ultimate methane production for the different sludge studied in this work.

System	SRT (d)	Ultimate methane production (NL CH_4·kg^{-1}VS-added)
HRAS	1.2	275.6 ± 7.4
HRSBR	0.8	307.8 ± 6.7
	2.0	187.2 ± 4.2

the lowest SRT (0.8 d) and the lowest BMP (187.2 ± 4.2 L CH_4·kg^{-1}VS-added) was obtained for the sludge generated at SRT of 2 d (both from the HRSBR). This observation is in agreement with the reported hypothesis of anaerobic degradability of the sludge increase when decreasing the SRT [36]. Finally, the sludge generated in the HRAS at SRT = 1.2d had a BMP of 275.6 ± 7.4 L CH_4·kg^{-1}VS-added (Table 7). Therefore, no quantitative differences were observed in terms of BMP between the two high rate systems. The BMP values obtained in this study were lower than those obtained by Ge et al. [19] (335.5 ± 8.7 and 357 ± 12.8 L CH_4·kg^{-1}VS-added) for the same SRT interval (2-1 d).

3.8. Energy balance

MRI and ERI were the two energy-based indices used to estimate the potential upgrade in energy recovery in our system. MRI provides the efficiency of the transformation of COD in the influent to methane, but without considering the COD removal efficiency, while ERI represents the fraction of energy that could be recovered from the influent. Considering, as detailed in the introduction of this work, that the energy content of wastewater is usually around 3–5 times higher than that needed for its treatment, an ERI value in the range 0.2–0.3 kJ_{CH4}·kJ_{INF}^{-1} would provide enough energy for WWTP autarky. Moreover, due to the assumed CHP conversion efficiency, the maximum theoretical ERI would be limited to a maximum value of 0.35 kJ_{CH4}·kJ_{INF}^{-1}.

Fig. 10 compares the indices obtained in this work (period III of HRAS and periods IIIA and IIIB of the HRSBR) to those in Meerburg et al. [15] (marked with an asterisk) for different experimental systems: a conventional AS, two HRSBRs, a contact stabilisation (CS) system and two high-rate contact stabilisation (HRCS) systems. The idea beneath CS is to enhance sorption and storage process when removing organic matter. In short, in a CS system, part of the sludge of the external recycle is aerated for its stabilisation. Then, this stabilised sludge is mixed for the influent under anoxic conditions and very short HRT to boost substrate sorption without high mineralization. Subjecting the sludge to feast and famine phases increases the selective pressure to favour storage and sorption processes.

As can be observed in Fig. 10, the high-rate systems (i.e. those operating at low SRTs) have at least three times higher MRI and ERI than those operating at higher SRTs. This agrees with the hypothesis of the high-rate systems that are designed to boost energy recovery from wastewaters. HRAS and HRSBR systems are in the ERI range of 0.18–0.28 kJ_{CH4}·kJ_{INF}^{-1} and hence seem able to provide WTTP autarky. Its values are only outperformed by the operation of some HRCS systems, but this technology also shows an important variability with lower

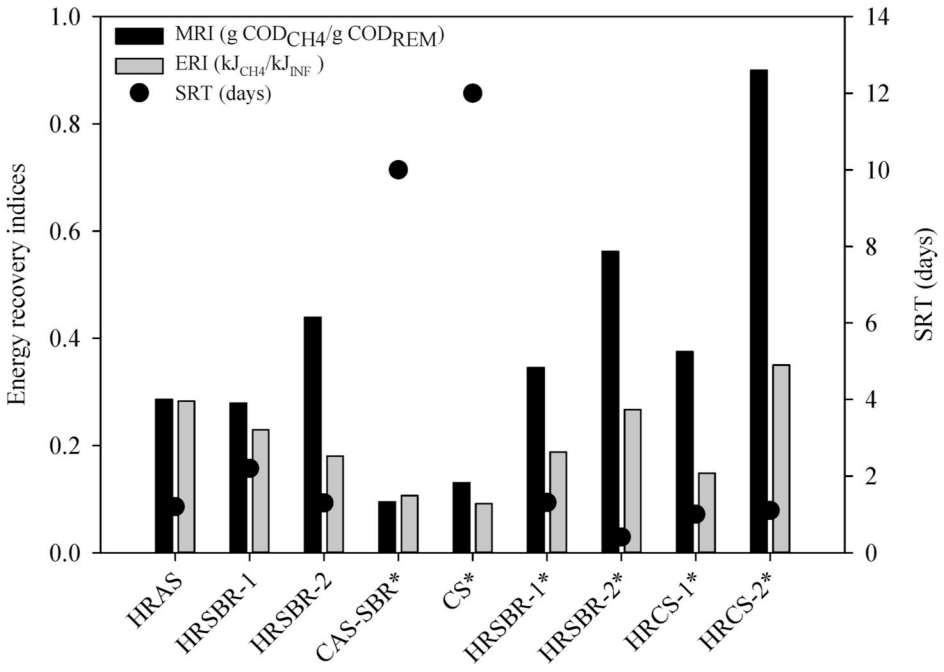

Fig. 10. Energy recovery indices obtained in this work compared to those obtained in Meerburg et al. [15] (indicated with an asterisk) for different configurations. HRAS corresponds to data from period III of the HRAS, and HRSBR-1 and HRSBR-2 to data from periods IIIA and IIIB of the HRSBR.

performance as observed for HRCS-1*. The differences observed between both HRCSs lay on the contact and stabilisation times. According to the authors, these parameters should be further optimized together with SRT and sludge separation.

When comparing continuous (HRAS) and SBR systems at similar SRT, the results show that the latter have higher MRI and thus, a higher energy recovery is obtained per gram of COD removed. However, the ERI is lower. This is correlated to the abovementioned observation of a higher percentage of COD removal in the HRAS. In fact, the ERI for the HRAS (0.283) is not that different from those obtained in the HRCS (0.15–0.35), which show much higher MRI. Thus, HRSBR systems should focus on increasing the amount of COD removed in order to be more competitive in this aspect.

3.9. Overall comparison

A dilemma arises between the two high-rate systems tested in this work. On the one hand, better results were obtained with the HRAS in terms of COD removal, ERI and solids concentration in the reactor. On the other hand, the HRSBR was better to avoid nitrification, provided better settleability and the extent of mineralization was lower, leading to a better MRI. However, the ERI was lower, but the COD removal efficiency and thus, the ERI, could be improved by increasing the oxygen transfer with better mixing conditions or by lengthening the aerobic phase. Therefore, the HRSBR seems to be a promising option, although an optimization of the cycle configuration is recommended to demonstrate the feasibility and reliability of the HRSBR as an A-stage in an A/B configuration.

4. Conclusions

A continuous HRAS was compared to a HRSBR under different operational conditions and the following conclusions were drawn:

- The continuous HRAS system provided higher COD removal efficiencies for all fractions, but the operation led to poorer sludge settleability.
- COD mineralization was calculated for the perfect settling scenario, obtaining values around 20–48% for the HRSBR, and 41–58% for the HRAS. However, the lower COD removal in the HRSBR led to lower overall energy recovery for this reactor (ERI = 0.283 and 0.229, for HRAS and HRSBR, respectively).
- Nitrification was more easily repressed in the HRSBR. This is an important factor to guarantee a suitable ammonia influent concentration for the subsequent B-stage.
- Similar BMP values were obtained for sludge in both systems under similar SRT conditions, with values in the range of 187–308 NL $CH_4 \cdot kg^{-1}VS$.
- Similar solids content in the effluent was observed for both systems. Obtaining low COD content and solids presence in the effluent is an essential feature of an A-stage system, since they affect the performance of the B-stage. Biomass separation should be improved in high-rate systems to allow maximum redirection of COD to anaerobic digestion.
- Values of Y_{OBS} higher than 1 were obtained for both systems, indicating that other non-biological processes (such as adsorption) occurred. Consequently, a fraction of COD was adsorbed in the solids of the effluent, leading to biomass concentration overestimation.

Acknowledgements

This work was supported by the Spanish Ministerio de Economía y Competitividad (CTQ2017-82404-R) with funds from the Fondo Europeo de Desarrollo Regional (FEDER). Natalia Rey is grateful for the PIF PhD grant funded by the Universitat Autònoma de Barcelona. The authors are members of the GENOCOV research group (Grup de Recerca Consolidat de la Generalitat de Catalunya, 2017SGR 1175, www.genocov.com).

References

[1] M.C.M. van Loosdrecht, D. Brdjanovic, Anticipating the next century of wastewater treatment, Science (80-.) 344 (2014) 1452–1453, https://doi.org/10.1126/science.1255183.

[2] I. Akanyeti, H. Temmink, M. Remy, A. Zwijnenburg, Feasibility of bioflocculation in a high-loaded membrane bioreactor for improved energy recovery from sewage, Water Sci. Technol. 61 (2010) 1433–1439, https://doi.org/10.2166/wst.2010.032.
[3] B. Kartal, J.G. Kuenen, M.C.M. Van Loosdrecht, Sewage treatment with anammox, Science 328 (2010) 702–703, https://doi.org/10.1126/science.1185941, 80.
[4] Y. Gu, Y. Li, X. Li, P. Luo, H. Wang, Z.P. Robinson, X. Wang, J. Wu, F. Li, The feasibility and challenges of energy self-sufficient wastewater treatment plants, Appl. Energy 204 (2017) 1463–1475, https://doi.org/10.1016/j.apenergy.2017.02.069.
[5] W. Verstraete, S.E. Vlaeminck, ZeroWasteWater: short-cycling of wastewater resources for sustainable cities of the future, Int. J. Sustain. Dev. World Ecol. 18 (2011) 253–264, https://doi.org/10.1080/13504509.2011.570804.
[6] J. Wan, J. Gu, Q. Zhao, Y. Liu, COD capture: a feasible option towards energy self-sufficient domestic wastewater treatment, Sci. Rep. 6 (2016) 1–9, https://doi.org/10.1038/srep25054.
[7] B. Korth, T. Maskow, S. Günther, F. Harnisch, Estimating the energy content of wastewater using combustion calorimetry and different drying processes, Front. Energy Res 5 (2017) 23. https://www.frontiersin.org/article/10.3389/fenrg.2017.00023.
[8] E.S. Heidrich, T.P. Curtis, J. Dolfing, Determination of the Internal Chemical Energy of Wastewater 45 (2011) 827–832, https://doi.org/10.1021/es103058w.
[9] I. Shizas, D.M. Bagley, M. Asce, Experimental Determination of Energy Content of Unknown Organics in Municipal Wastewater Streams, vol. 130, 2005.
[10] A. AlSayed, M. Soliman, A. Eldyasti, Anaerobic-based water resources recovery facilities: a review, Energies 13 (2020), https://doi.org/10.3390/en13143662.
[11] P.L. McCarty, J. Bae, J. Kim, Domestic wastewater treatment as a net energy producer–can this be achieved? Environ. Sci. Technol. 45 (2011) 7100–7106, https://doi.org/10.1021/es2014264.
[12] A.I. Versprille, B. Zuurveen, T. Stein, The A–B process: a novel two stage wastewater treatment system, Water Sci. Technol. 17 (1985) 235–246.
[13] Y.J. Liu, J. Gu, Y. Liu, Energy self-sufficient biological municipal wastewater reclamation: present status, challenges and solutions forward, Bioresour. Technol. 269 (2018) 513–519, https://doi.org/10.1016/j.biortech.2018.08.104.
[14] G. Xu, H. Wang, J. Gu, N. Shen, Z. Qiu, Y. Zhou, Y. Liu, A novel A-B process for enhanced biological nutrient removal in municipal wastewater reclamation, Chemosphere 189 (2017) 39–45, https://doi.org/10.1016/j.chemosphere.2017.09.049.
[15] F.A. Meerburg, N. Boon, T. Van Winckel, J.A.R. Vercamer, I. Nopens, S. E. Vlaeminck, Toward energy-neutral wastewater treatment: a high-rate contact stabilization process to maximally recover sewage organics, Bioresour. Technol. 179 (2015) 373–381, https://doi.org/10.1016/j.biortech.2014.12.018.
[16] B. Wett, P. Aichinger, M. Hell, M. Andersen, L. Wellym, Y. Fukuzaki, Y.S. Cao, G. Tao, J. Jimenez, I. Takacs, C. Bott, S. Murthy, Operational and structural A-stage improvements for high-rate carbon removal, Water Environ. Res. (2020) 1354, https://doi.org/10.1002/wer.1354, wer.
[17] J. Smitshuijzen, J. Pérez, O. Duin, M.C.M. van Loosdrecht, A simple model to describe the performance of highly-loaded aerobic COD removal reactors, Biochem. Eng. J. 112 (2016) 94–102, https://doi.org/10.1016/j.bej.2016.04.004.
[18] J. Jimenez, M. Miller, C. Bott, S. Murthy, H. De Clippeleir, B. Wett, High-rate activated sludge system for carbon management - evaluation of crucial process mechanisms and design parameters, Water Res. 87 (2015) 476–482, https://doi.org/10.1016/j.watres.2015.07.032.
[19] H. Ge, D.J. Batstone, M. Mouiche, S. Hu, J. Keller, Nutrient removal and energy recovery from high-rate activated sludge processes – impact of sludge age, Bioresour. Technol. 245 (2017) 1155–1161, https://doi.org/10.1016/j.biortech.2017.08.115.
[20] I. Sancho, S. Lopez-Palau, N. Arespacochaga, J.L. Cortina, New concepts on carbon redirection in wastewater treatment plants: a review, Sci. Total Environ. 647 (2019) 1373–1384, https://doi.org/10.1016/j.scitotenv.2018.08.070.
[21] Y. Jiang, L. Wei, H. Zhang, K. Yang, H. Wang, Removal performance and microbial communities in a sequencing batch reactor treating hypersaline phenol-laden wastewater, Bioresour. Technol. 218 (2016) 146–152, https://doi.org/10.1016/j.biortech.2016.06.055.
[22] M.C. Tomei, J. Soria Pascual, D. Mosca Angelucci, Analysing performance of real textile wastewater bio-decolourization under different reaction environments, J. Clean. Prod. 129 (2016) 468–477, https://doi.org/10.1016/j.jclepro.2016.04.028.
[23] M. Sekine, S. Akizuki, M. Kishi, T. Toda, Stable nitrification under sulfide supply in a sequencing batch reactor with a long fill period, J. Water Process Eng. 25 (2018) 190–194, https://doi.org/10.1016/j.jwpe.2018.05.012.
[24] I. Angelidaki, M. Alves, D. Bolzonella, L. Borzacconi, J.L. Campos, A.J. Guwy, S. Kalyuzhnyi, P. Jenicek, J.B. van Lier, Defining the biomethane potential (BMP) of solid organic wastes and energy crops: a proposed protocol for batch assays, Water Sci. Technol. 59 (2009) 927–934, https://doi.org/10.2166/wst.2009.040.
[25] D. Mamais, D. Jenkins, P. Prrr, A rapid physical-chemical method for the determination of readily biodegradable soluble COD in municipal wastewater, Water Res. 27 (1993) 195–197, https://doi.org/10.1016/0043-1354(93)90211-Y.
[26] APHA, Standard Methods for the Examination of Water and Wastewater, 1995, 19th Editi.
[27] A. Rahman, H. De Clippeleir, W. Thomas, J.A. Jimenez, B. Wett, A. Al-Omari, S. Murthy, R. Riffat, C. Bott, A-stage and high-rate contact-stabilization performance comparison for carbon and nutrient redirection from high-strength municipal wastewater, Chem. Eng. J. 357 (2019) 737–749, https://doi.org/10.1016/j.cej.2018.09.206.
[28] W. Rössle, W. Pretorius, A review of characterisation requirements for in-line prefermenters: paper 1: wastewater characterisation, WaterSA 27 (2001) 405–412, https://doi.org/10.4314/wsa.v27i3.4985.
[29] A. Rahman, F.A. Meerburg, S. Ravadagundhi, B. Wett, J. Jimenez, C. Bott, A. Al-Omari, R. Riffat, S. Murthy, H. De Clippeleir, Bioflocculation management through high-rate contact-stabilization: a promising technology to recover organic carbon from low-strength wastewater, Water Res. 104 (2016) 485–496, https://doi.org/10.1016/j.watres.2016.08.047.
[30] L. Faust, H. Temmink, A. Zwijnenburg, A.J.B. Kemperman, H.H.M. Rijnaarts, High loaded MBRs for organic matter recovery fromsewage: effect of solids retention time on bioflocculation and on the role of extracellular polymers, Water Res. 56 (2014) 258–266, https://doi.org/10.1016/j.watres.2014.03.006.
[31] A. Rahman, T. Wadhawan, E. Khan, R. Riffat, I. Takács, H. De Clippeleir, B. Wett, J. A. Jimenez, A. Al-Omari, S. Murthy, Characterizing and quantifying flocculated and adsorbed chemical oxygen demand fractions in high-rate processes, Glob. Challenges Sustain. Wastewater Treat. Resour. Recover. IWA Spec. Conf. (2014), https://doi.org/10.1103/PhysRevB.91.155112.
[32] M.W. Miller, J. De Armond, M. Elliot, M. Kinyua, D. Kinnear, B. Wett, S. Murthy, C. B. Bott, Settling and dewatering characteristics of an A-stage activated sludge process proceeded by shortcut biological nitrogen removal, Int. J. Water Wastewater Treat. 2 (2016), https://doi.org/10.16966/2381-5299.133.
[33] M.S.I. Mozumder, C. Picioreanu, M.C.M. Van Loosdrecht, E.I.P. Volcke, Effect of heterotrophic growth on autotrophic nitrogen removal in a granular sludge reactor, Environ. Technol. 35 (2014) 1027–1037, https://doi.org/10.1080/09593330.2013.859711.
[34] T. Van Winckel, X. Liu, S.E. Vlaeminck, I. Takács, A. Al-Omari, B. Sturm, B. V. Kjellerup, S.N. Murthy, H. De Clippeleir, Overcoming floc formation limitations in high-rate activated sludge systems, Chemosphere 215 (2019) 342–352, https://doi.org/10.1016/j.chemosphere.2018.09.169.
[35] M. Henze, C.P.L. Grady, W. Gujer, G.v.R. Marais, T. Matsuo, Activated sludge model No . 1, IAWPRC Sci. c Tech. Reports. 1223 (1987) 19–21, https://doi.org/10.1016/S0273-1223(98)00785-9.
[36] H. Ge, D.J. Batstone, J. Keller, Operating aerobic wastewater treatment at very short sludge ages enables treatment and energy recovery through anaerobic sludge digestion, Water Res. 47 (2013) 6546–6557, https://doi.org/10.1016/j.watres.2013.08.017.